Electronic Supplementary Material (ESI) for CrystEngComm.

Polyoxometalates Templated Silver-bisphosphine Sandwich: Structurally Tunable Hybrid Materials

Sheng-Jie Yao, Zhen-Qing Qi, Zhan-Guo Jiang*, and Cai-Hong Zhan*

Key Laboratory of the Ministry of Education for Advanced Catalysis Material, Institute of Physical Chemistry, College of Chemistry and Materials Science, Zhejiang Normal University, Jinhua 321004, China.

Email: jzg@zjnu.cn; chzhan@zjnu.cn

Powder X-ray Diffraction (PXRD)

Powder XRD patterns were obtained using a Bruker D8 Advance X-ray diffractometer with (λ (CuKα) = 1.5405 Å) radiation.

Fourier Transform Infrared Spectroscopy (FTIR)

The materials were recorded on KBr disk using a Nicolet NEXUS 670 spectrometer between 500 and 4000 cm^{-1}.

Thermogravimetric Analyses (TGA)

They were carried out on a TA Instruments STA499 F5 thermobalance with a 100 $mL \cdot min^{-1}$ flow of nitrogen; the temperature was ramped from 20 °C to 800 °C at a rate of 10 $°C \cdot min^{-1}$.

Single-crystal X-ray Diffraction (SCXRD)

The suitable crystals of the four compounds were mounted in a Hampton cryoloop with Paratone® N oil cryoprotectant. Intensity data collections were carried out at T = 293 or 273 K with a Bruker D8 VENTURE diffractometer equipped with a PHOTON 100 CMOS bidimensional detector using a high brilliance IμS microfocus X-ray Mo Ka monochromatized radiation (λ = 0.71073 Å) and Cu Ka monochromatized radiation (λ = 1.54178 Å). With the aid of Olex2, the structure was solved with the ShelXT structure solution program using Intrinsic Phasing and refined with the ShelXL refinement package using Least Squares minimization. Further details about of the crystal structure determinations may be obtained free of charge via the Internet at https://www.ccdc.cam.ac.uk/ CCDC 2326041, 2326044-2326046.

Cyclic Voltammetry (CV)

Cyclic voltammetry (CV) experiments were carried out at room temperature in $CHCl_3$ on an electrochemical station (CHI 660E, China). All CV experiments were performed using a glassy carbon (GC) electrode with a diameter of 3 mm as the working electrode. The electrode surface was polished routinely with 0.05 μm alumina–water slurry on a felt surface immediately before use. The counter electrode was a Pt wire and the reference electrode was an Ag/AgCl (KCl-saturated).

Materials and reagents

All starting materials and regents were purchased from commercial suppliers and used without further purification. $AgNO_3$, CH_3CN(AR) and CH_2Cl_2 (AR) were purchased from Sinopharm Chemical Reagent Co., Ltd., China. Precursors like $[N(C_4H_9)_4]_4[Mo_8O_{26}]$、$[N(C_4H_9)_4]_2[Mo_6O_{19}]$、$[N(C_4H_9)_4]_3[PW_{12}O_{40}]$、$[N(C_4H_9)_4]_3[PMo_{12}O_{40}]$ are synthesized according to the method in reference. These compounds were all synthesized according to the liquid phase diffusion method.

Synthesis and Experimental Section.

The synthesis of $Ag_2(dppp)_2(NO_3)_2$:

A mixture of $AgNO_3$(0.0067g,0.04mmol) dissolved in 5 ml acetonitrile and 1,3-double (diphenylphosphine) propane (dppp) (0.016 g, 0.04 mmol) dissolved in 3 ml CH_2Cl_2. The colorless bulk crystals were volatilized at room temperature for 3-4 days.

The synthesis of $Ag_4(dppp)_4(Mo_8O_{26})$ (1):

$(NH_4)_6[MnMo_9O_{32}]\cdot 8H_2O$ (0.05 mmol) was stirred to dissolve in 10 ml water, adding tetrabutyl ammonium hydroxide (1 mmol) and stirring quickly. We found a brown precipitate, after filterring and being vacuum dried, we should add 5 ml acetonitrile to dissolve the powder. A mixture of $AgNO_3$(0.04 mmol) dissolved in 5 ml acetonitrile and 1,3-double (diphenylphosphine) propane (dppp) (0.04 mmol) dissolved in 3 ml CH_2Cl_2, then the three solutions were mixed and stirred together. The colorless bulk crystals were volatilized at room temperature for 3-4 days. Yield: 50.2% (based on $(NH_4)_6[MnMo_9O_{32}]\cdot 8H_2O$). Elemental analysis theory%: H, 3.7; C, 43.2; N, 1.7; Actual: H, 3.5; C, 41; N, 1.6. Compound 1 is also obtained by reacting $[N(C_4H_9)_4]_4[Mo_8O_{26}]$ with $AgNO_3$, dppp in a mixture of acetonitrile and dichloromethane in a molar ratio of 1:4:4. Yield: 80.5% (based on $[N(C_4H_9)_4]_4[Mo_8O_{26}]$).

The synthesis of $[Ag_4(dppp)_4(\alpha\text{-}PW_{12}O_{40})]NO_3$ (2):

$[N(C_4H_9)_4]_3[PW_{12}O_{40}]$ (0.01 mmol) and 5ml acetonitrile was stirred in a 20ml glass bottle with a magnetic stirring bar until the solid is completely dissolved. A mixture of $AgNO_3$(0.04mmol) dissolved in 5ml acetonitrile and 1,3-double (diphenylphosphine) propane (dppp) (0.04 mmol) dissolved in 3 ml CH_2Cl_2, and the colorless bulk crystals were volatilized at room temperature for 3-4 days. Yield: 82.9% (based on $[N(C_4H_9)_4]_3[PW_{12}O_{40}]$). Elemental analysis theory%: H, 2.1; C, 25.8; N, 0.28; Actual: H, 2.7; C, 27; N, 0.34.

The synthesis of$Ag_3(dppp)_3(PMo_{12}O_{40})$ (3):

$[N(C_4H_9)_{4]3}[PMo_{12}O_{40}]$ (0.01 mmol) and 5ml acetonitrile was stirred in a 20ml glass bottle with a magnetic stirring bar until the solid is completely dissolved. A mixture of $AgNO_3$(0.04mmol) dissolved in 5 ml acetonitrile and 1,3-double (diphenylphosphine) propane (dppp) (0.04 mmol) dissolved in 5 ml CH_2Cl_2, and the light brown crystals were volatilized at room temperature for 3-4 days. Yield: 88.7% (based on

$[N(C_4H_9)_4]_3[PMo_{12}O_{40}]$). Elemental analysis theory%: H, 2.9; C, 36.2; Actual: H, 2.7; C, 38.

The synthesis of $Ag_2(dppp)_2(CH_3CN)_2(Mo_6O_{19})$ (4):

$[N(C_4H_9)_4]_2[Mo_6O_{19}]$ (0.01 mmol) and 5ml acetonitrile was stirred in a 20ml glass bottle with a magnetic stirring bar until the solid is completely dissolved. A mixture of $AgNO_3$(0.0067g,0.04mmol) dissolved in 5 ml acetonitrile and 1,3-double (diphenylphosphine) propane (dppp) (0.04 mmol) dissolved in 3 ml CH_2Cl_2, and the yellow acicular crystal were volatilized at room temperature for 3-4 days. Yield: 89.1% (based on $[N(C_4H_9)_4]_4[Mo_8O_{26}]$). Elemental analysis theory%: H, 2.9; C, 34.3; N, 1.4; Actual: H, 3.2; C, 37; N, 1.5.

Structure

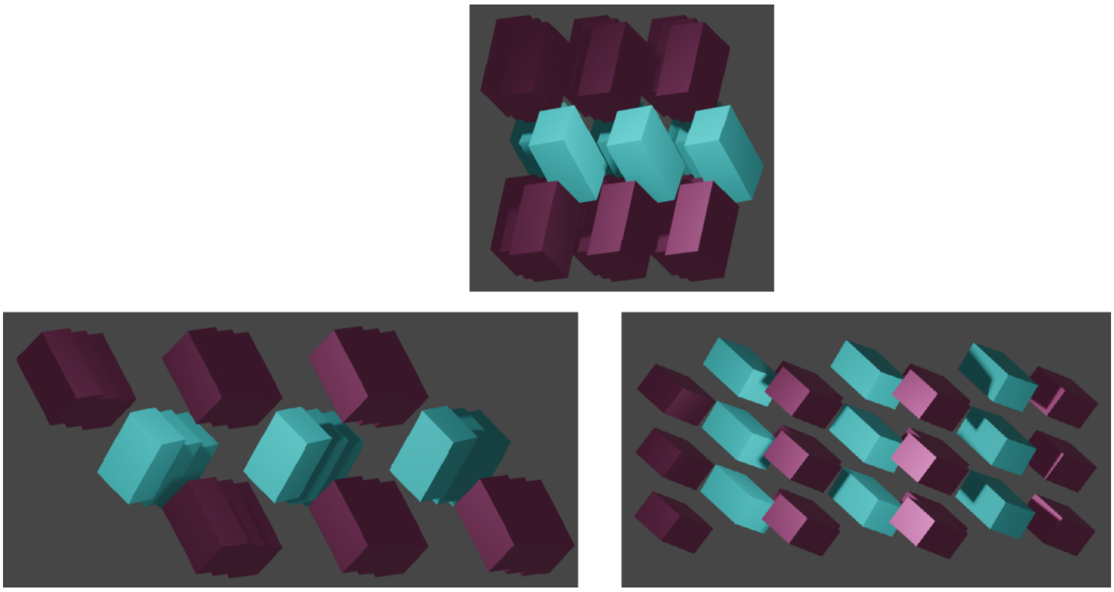

Figure S1. 3D brick stacking diagram of compound **1** in other directions.

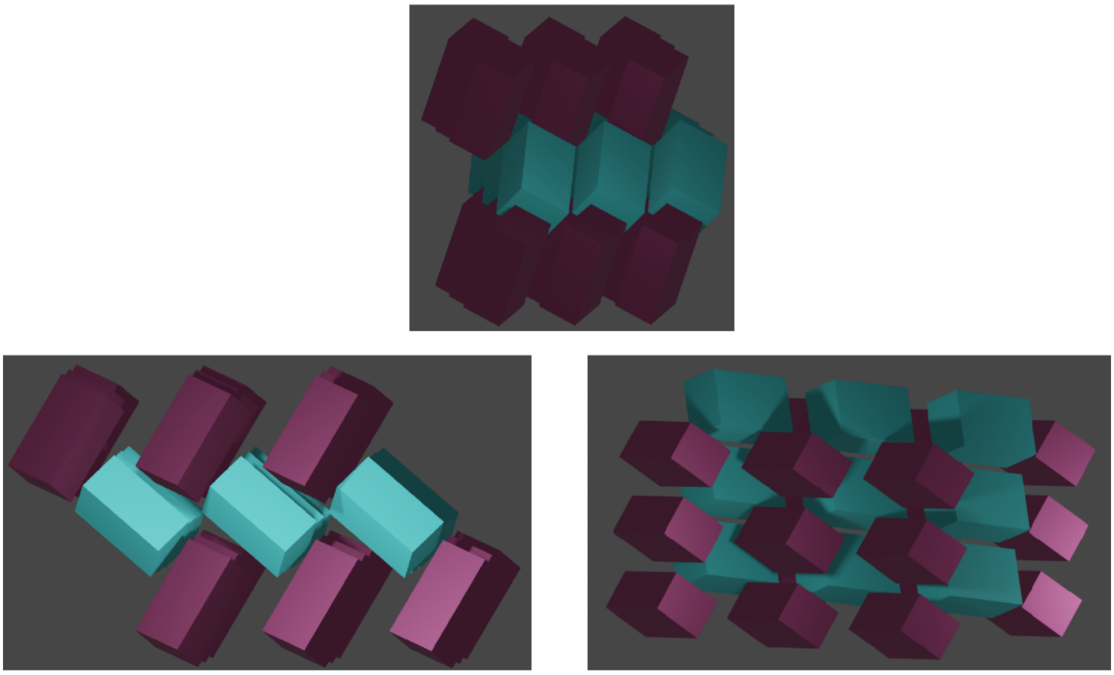

Figure S2. 3D brick stacking diagram of compound **2** in other directions.

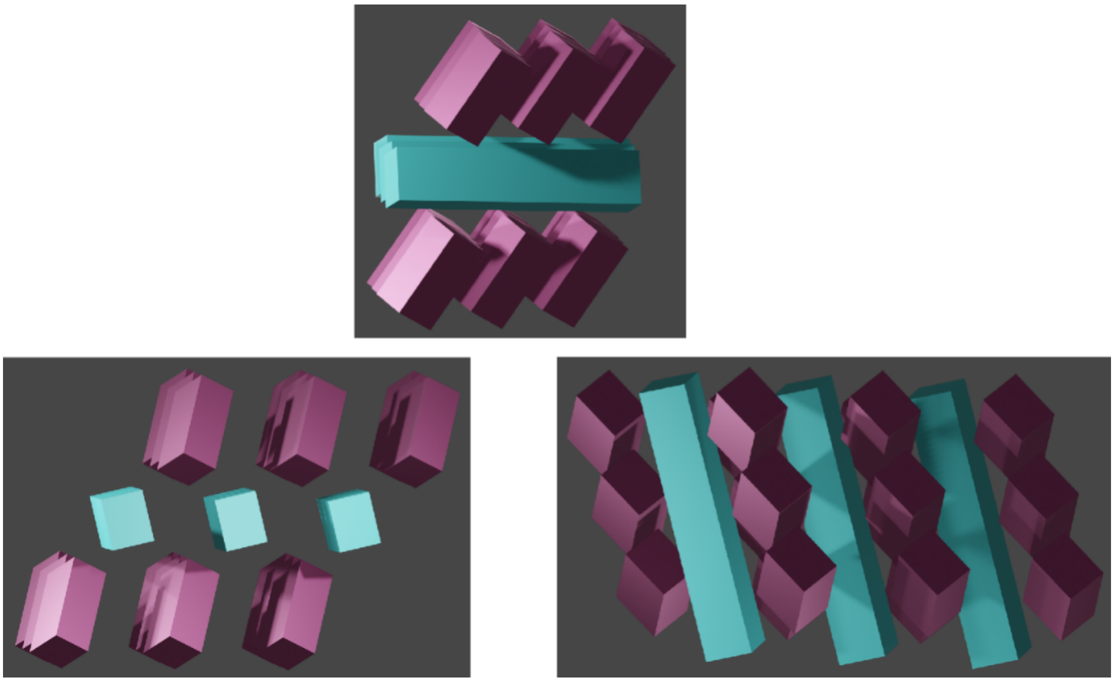

Figure S3. 3D brick stacking diagram of compound **3** in other directions.

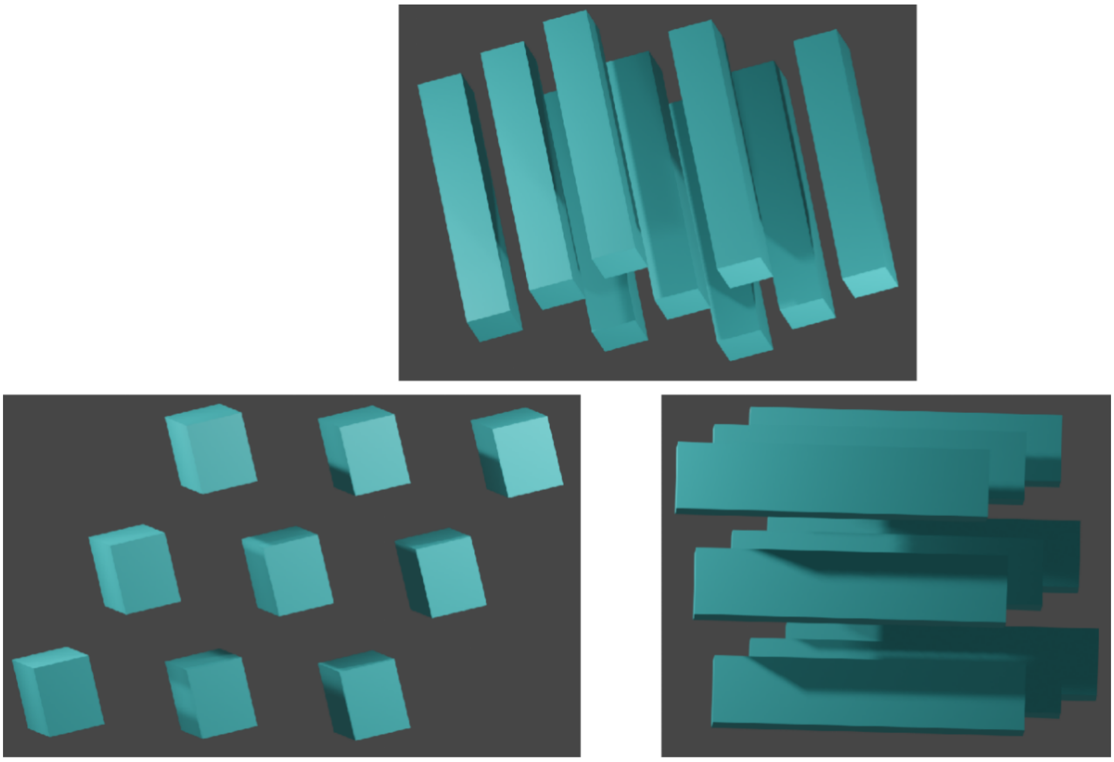

Figure S4. 3D brick stacking diagram of compound **4** in other directions.

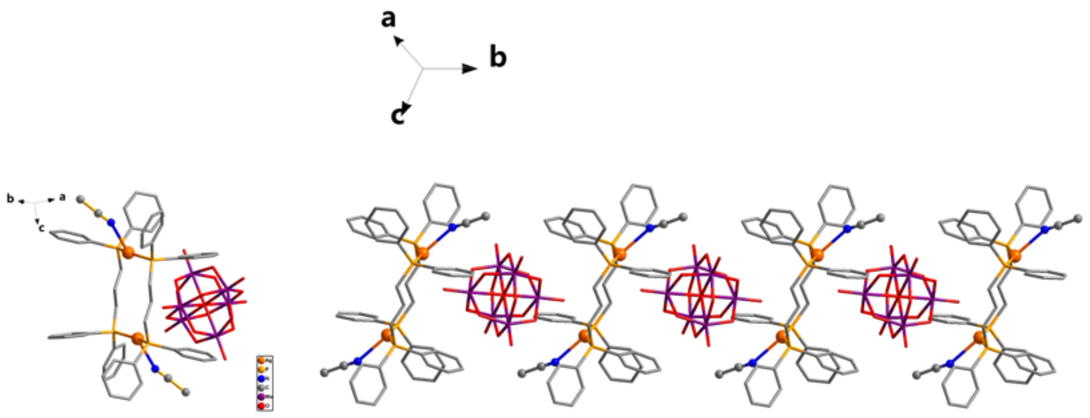

Figure S5. The two structures of compound **4** with solvent molecule acetonitrile are (a) individual molecules and (b) one-dimensional chains.

Table S1. Crystal data and structure refinement for the compounds **1**-**2**.

Complex	**1**	**2**
Empirical formula	$C_{118}H_{124}Ag_4Mo_8N_4O_{28}P_8$	$C_{108}H_{104}Ag_4O_{40}P_9W_{12}$
Formula weight	3492.96	4958.32
Temperature/K	293.00	273.15
Crystal system	monoclinic	monoclinic
Space group	$P2_1/n$	$P2_1/n$
a/Å	14.2663(4)	15.7042(10)
b/Å	20.3743(6)	22.4607(16)
c/Å	22.7754(5)	20.2442(15)
α/°	90	90
β/°	97.1750(10)	102.668(2)
γ/°	90	90
Volume/Å^3	6568.2(3)	6966.9(8)
Z	2	2
ρcalcg/cm^3	1.766	2.364
μ/mm^{-1}	1.484	10.580
F(000)	3456.0	4566.0
Radiation	MoKα (λ = 0.71073)	MoKα (λ =0.71073)
2Θ range for data collection/°	4.386 to 52.804	4.496 to 51.364
Index ranges	$-17 \leqslant h \leqslant 17, -25 \leqslant k \leqslant 22, -28 \leqslant l \leqslant 27$	$-19 \leqslant h \leqslant 19, -27 \leqslant k \leqslant 27, -24 \leqslant l \leqslant 24$
Reflections collected	44774	92378
Independent reflections	13449 [R_{int} = 0.0411, R_{sigma} = 0.0393]	13212 [R_{int} = 0.1065, R_{sigma} = 0.0586]
Data/restraints/parameters	13449/97/799	13212/1014/703
Goodness-of-fit on F^2	1.044	1.040
Final R indexes[I>=2σ(I)]	R_1 = 0.0295, wR_2 = 0.0695	R_1 = 0.0656, wR_2 = 0.1911
Largest diff. peak/hole / e Å^{-3}	0.49/-0.58	1.85/-3.26

Table S2. Crystal data and structure refinement for the compounds **3**-**4**.

Complex	**3**	**4**
Empirical formula	$C_{162}H_{156}Ag_6Mo_{24}O_{80}P_{14}$	$C_{58}H_{58}Ag_2Mo_6N_2O_{19}P_4$
Formula weight	6766.22	2002.32
Temperature/K	297.00	293.0
Crystal system	triclinic	triclinic
Space group	*P*-1	*P*-1
a/Å	14.0626(4)	11.6266(10)
b/Å	14.8889(3)	12.7787(12)
c/Å	27.6698(7)	13.6690(13)
α/°	100.6530(10)	109.407(3)
β/°	93.370(2)	96.054(3)
γ/°	109.7070(10)	115.217(3)
Volume/Å^3	5314.0(2)	1658.7(3)
Z	1	1
ρcalcg/cm^3	2.114	2.005
μ/mm^{-1}	17.179	1.840
F(000)	3268.0	978.0
Radiation	CuKα (λ = 1.54178)	MoKα (λ =0.71073)
2Θ range for data collection/°	6.46 to 160.312	4.42 to 52.802
Index ranges	$-17 \leqslant h \leqslant 17, -14 \leqslant k \leqslant 18, -35 \leqslant l \leqslant 34$	$-14 \leqslant h \leqslant 14, -15 \leqslant k \leqslant 15, -17 \leqslant l \leqslant 17$
Reflections collected	77753	26690
Independent reflections	22600 [R_{int} = 0.0792, R_{sigma} = 0.0707]	6723 [R_{int} = 0.0327, R_{sigma} = 0.0271]
Data/restraints/parameters	22600/468/1315	6723/0/413
Goodness-of-fit on F^2	1.033	1.164
Final R indexes[I>=2σ(I)]	R_1 = 0.0666, wR_2 = 0.1547	R_1 = 0.0238, wR_2 = 0.0667
Largest diff. peak/hole / e Å^{-3}	1.39/-1.86	1.10/-0.91

Table S3. Bond Distances (Å) and Angles (deg) for compounds **1**-**4**.

assignment	compounds			
	1	**2**	**3**	**4**
O-Ag	2.7221 (22)	2.6299(157)	3.2545(104)	2.7512(31)
Mo-O-Ag W-O-Ag	142.018(107)	120.758（684)	138.455（408)	129.878(139)
O-Ag-Ag	60.195 (45)	27.337(308)	48.565(178)	52.734(54)

Table S4. The ^{31}P peaks shift of four compounds in solution relative to [Ag$_2$dppp$_2$].

	compounds			
	1	**2**	**3**	**4**
Main peaks	1.65 ppm and 4.64 ppm	1.70 ppm and 3.78ppm	0.86 ppm and 4.10 ppm	3.29 ppm and 6.35 ppm
Shift compared to [Ag$_2$dppp$_2$]	0.26 ppm and 1.20 ppm	0.31 ppm and 0.34 ppm	0.53 ppm and 0.66 ppm	1.90 ppm and 2.91 ppm

Powder X-ray diffraction (PXRD)

The Powder X-ray diffraction (PXRD) patterns for compounds **1-4** can be compared with the simulated pattern obtained from the X-ray single-crystal diffraction analysis. Their peak positions are in good agreement with each other, indicating the phase purity of the products. The differences in intensity may be due to the preferred orientation of the powder samples.

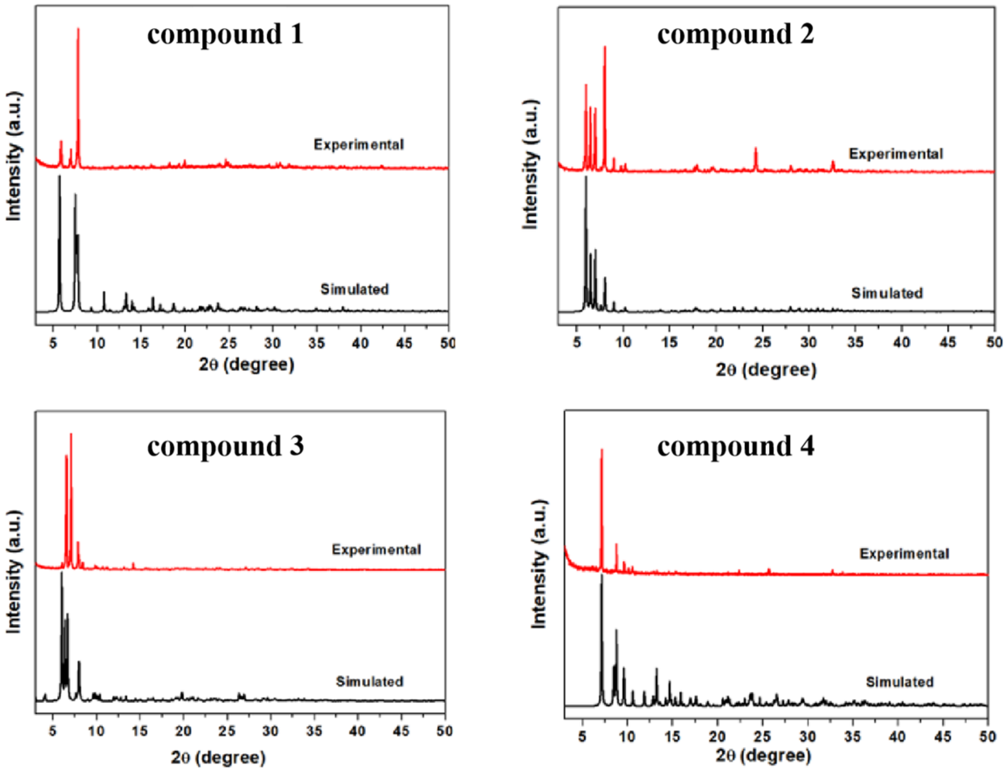

Figure S6. PXRD pattern of compounds **1-4**.

Fourier Transform Infrared Spectroscopy (FTIR)

The C-H stretching vibration peak on the aromatic ring ranges from 2900 to 3100 cm^{-1}. The C-H stretching vibration peak on the benzene ring ranges from 1430 to 1480 cm^{-1}. The absorption peak near 740 cm^{-1} originates from the out of plane bending vibration of C-H. The peak between 420 and 520 cm^{-1} belongs to the out of plane bending vibration of the ring in substituted benzene. Asymmetric stretching vibration absorption peak of Mo-O$_b$-Mo bond at 665 cm^{-1}. The four peaks of 698, 744, 833, and 921 cm^{-1} belong to the asymmetric stretching vibration of Mo-O$_b$.The characteristic peak of $\{PW_{12}\}$ ranges from 804 to 1065 cm^{-1}, while the characteristic peak of $\{PMo_{12}\}$ ranges from 808 to 1060 cm^{-1}. The peaks between 500 and 900 cm^{-1} correspond to the peaks of Mo-O$_t$ and Mo-O$_b$-Mo in $\{Mo_6\}$ and $\{Mo_8\}$.

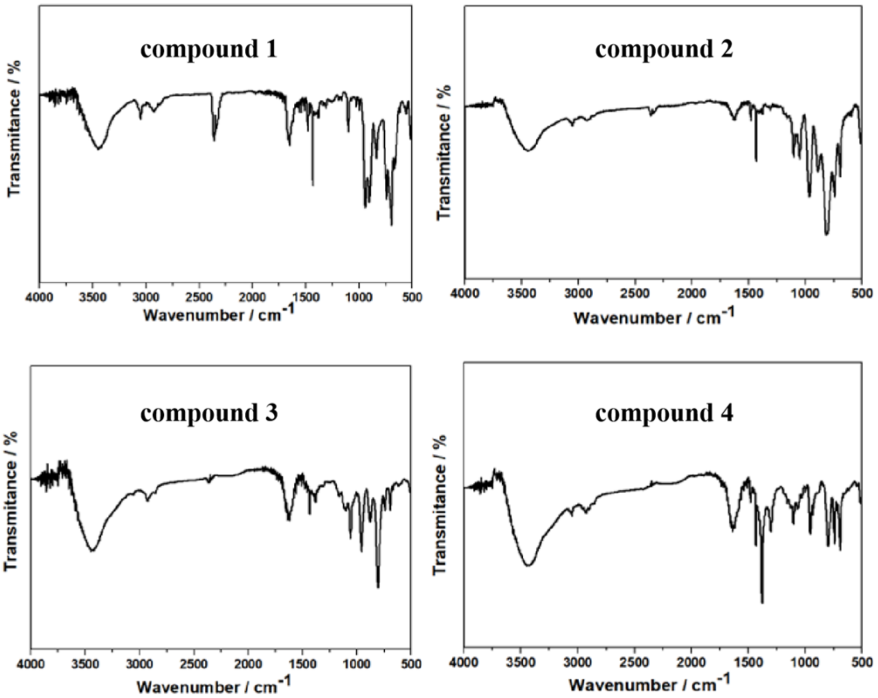

Figure S7. IR spectra of compound **1-4**.

Thermogravimetric analyses (TGA)

As shown in Figure S8, Compound **1** has a total weight loss of 50% corresponding with the loss of dppp organic ligands in the range of 50~600 °C (Theory: 47.23 %). Compound **2** has a weight loss of the compound was 20 % in the range of 50~600 °C, which mainly due to the decomposition of dppp organic ligands (Theory: 24.27 %). Compound **3** had a total weight loss of 20 % corresponding with the loss of dppp organic ligands when the temperature was 320~600 °C (Theory: 18.29 %). Compound **4** had a weight loss of 4% in the range of 50~260 °C because of the decomposition of CH_3CN (Theory: 4.0 %), and further a weight loss of 37% corresponding with the loss of dppp organic ligands when the temperature is 260~600 °C (Theory: 41.2%).

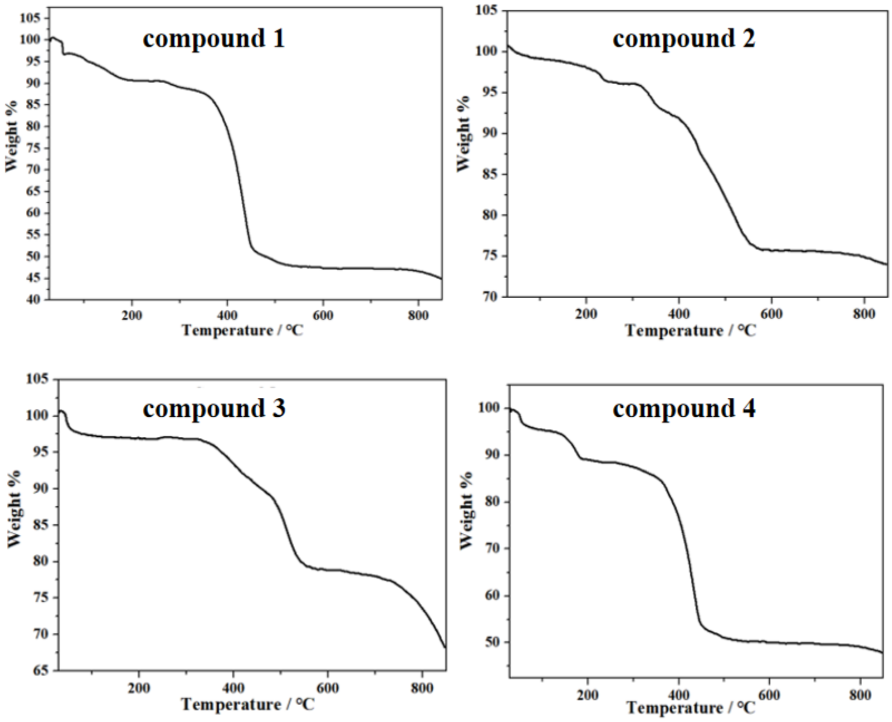

Figure S8. Thermogravimetric analysis trace of compounds **1-4**.

Electrochemistry

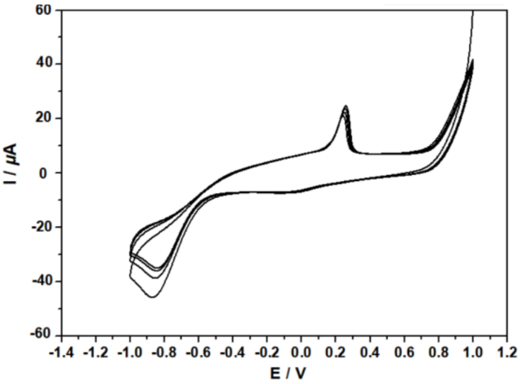

Figure S9. Cyclic voltammogram of [Ag_2dppp_2] at a scan rate of 50 mV s^{-1}.